

Short Communication

Electrochemical Sensor Based on Glassy Carbon Electrode Modified by Palladium Doped ZnO Nanostructures for Glucose Detection

Qingshan Yuan¹, Zunju Zhang^{2,*}, Lei Li¹

¹ Northeast Petroleum University, Department of petroleum and chemical engineering, Qinhuangdao, Hebei 066004, China

² Hebei University of Environmental Engineering, Qinhuangdao, Hebei 066004, China

*E-mail: zhangzunju@sina.com

Received: 13 February 2020 / Accepted: 5 April 2020 / Published: 10 May 2020

An electrochemical glucose sensor based on a glassy carbon electrode (GCE) decorated by palladium (Pd) doped ZnO nanorods (NRs) was developed. The Pd-doped ZnO NRs were prepared by a facile chemical bath deposition technique, and the characterizations of the samples were studied by X-ray diffraction and scanning electron microscopy analysis. Electrochemical behaviors of the Pd-doped ZnO NRs/GCE electrode to glucose were determined by electrochemical impedance spectroscopy, cyclic voltammetry and differential pulse voltammetry. The electrochemical results indicated that the Pd-doped ZnO NRs/GCE revealed an excellent response to glucose with a detection limit of 0.3 μM and a sensitivity of 0.64 $\mu\text{A}/\mu\text{Mcm}^2$. This sensor was applied satisfactorily to glucose determination in blood serum samples. With remarkable electrochemical performance, Pd-doped ZnO NRs / GCE can provide a suitable platform in the manufacture of a variety of electrochemical sensors and have a great promise for sensing applications.

Keywords: Electrochemical glucose sensor; Doped ZnO nanostructures; Cyclic voltammetry; Differential pulse voltammetry

1. INTRODUCTION

Glucose serves to supply energy to the living cells and in biological systems, they act as a metabolic intermediate though high levels of glucose in the blood can cause diabetes mellitus, a condition that has been one of the topmost reasons to cause disability and death around the world [1, 2]. Hence it is quite necessary to fabricate highly efficient sensors to detect glucose quickly and reliably. This has led to numerous researches being done to develop enzyme based glucose sensors that can transfer electrons directly and has high stability and repeatability [3]. Glucose sensors without enzymes have been

developed in recent time using noble metals, transition metal oxides, and metal nanoparticles[4, 5]. But these sensors are expensive due to the price of the noble metals, besides having a narrow linear range and a very low selectivity of glucose because of the surface poisoning that occurs during the electrochemical process[6]. Therefore, it is of great interest to design a glucose sensor that is highly sensitive, selective, and low in cost to be employed in biomedical applications. In light of recent years, the electrochemical approach has been the possible choice to replace traditional instrument-based methods to directly determine the glucose level because of their compatibility to perform on-site detection[7, 8]. These methods are cost-effective, simple and fast. Differential pulse voltammetry technique based electrochemical detections showed a huge potential due to their better sensitivity, efficiency, and low detection profile[9]. Hence, they can be employed for a vast analyte spectrum.

The high specific surface area to volume ratio, high carrier transport, cost-effectiveness and simple synthesizing makes one-dimensional (1D) metal oxide semiconductor nanostructures like nanorods, nanotubes, and nanowires to draw much attention[10, 11]. In specific, 1D Zinc oxide nanostructures have been chosen because of their non-toxic nature, better biochemical stability, electron transfer, and a high isoelectric point[12, 13]. But, most of the investigations were based on Zinc oxide nanostructures with enzymes that were not stable and sensitive enough to detect glucose[14].

Here, we successfully fabricated a non-enzymatic biosensor based on palladium (Pd)-doped ZnONRs for glucose detection. The Pd-doped Zinc oxidenanorods were grown by chemical bath deposition method and were characterized by the X-ray diffraction and scanning electron microscopy. To prepare sensing electrodes, the Pd-doped ZnOnanorods were deposited onto a glassy carbon electrode (GCE) substrates. The electrochemical properties of the electrodes were considered by electrochemical impedance spectroscopy and cyclic voltammetry. It had indicated an excellent and specific performance with good selectivity, sensitivity, and low detection limit.

2. MATERIALS AND METHOD

A facile chemical bath deposition method was employed to prepare ZnOnanorods(NRs) array on a glassy carbon electrode (GCE). The surface of GCE was cleaned using DI water and polished with 0.1 μm alumina slurry. Radiofrequency sputtering was done using a customized sputtering unit and a 99.999% pure zinc oxide target to prepare zinc oxide nano seed layers to grow nanorods at ambient temperature. 25 mM $\text{Zn}(\text{CH}_3\text{CO}_2)_2$ and 24 mM $(\text{CH}_2)_6\text{N}_4$ were dissolved in deionized water to form the zinc acetate precursor solution. This solution was mixed in the reactor at 35⁰C and 1000 rpm. The seed layer on the GCE was placed into the precursor solution for 3 h at 95⁰ C to allow the synthesis of nanorods. Then the GCE was taken from the reactor. With careful consideration, the synthesized zinc oxide nanorods were washed with deionized water to remove the remaining salts and then dried in nitrogen at 80⁰C for 1 h before undergoing characterization. To prepare Pd-doped ZnONRs, the dopant precursor solution was modified. Separate dissolution of 1 wt% of $\text{Pd}(\text{C}_5\text{H}_7\text{O}_2)_2$ in 0.4 mol of isopropanol and DI water (with a 10:1 M ratio) was done, trailed by 30 min stir at ambient temperature. The resulting solution was added to the previous solution and the same procedure for undoped ZnONRs followed.

A field-emission scanning electron microscope (Hitachi FE-SEM S4800) was employed to study the structural features. An X'pert Pro X-ray diffractometer (PANalytical, NED), using Cu-K α radiation source ($\lambda = 1.5406 \text{ \AA}$) was used to generate X-ray diffraction (XRD) patterns. Electrochemical impedance spectroscopy (EIS) was done in 0.5 M H₂SO₄ containing 0.1 M KOH solution under 0.5 V. Nyquist plots were used to record with the frequency range of 100 kHz to 0.1 Hz. Cyclic voltammetry (CV) measurements were done in -0.1 to 1 V potential range at a 30 mVs⁻¹ scan rate in phosphate buffer at pH 7.4. Differential pulse voltammetry (DPV) measurements were employed in the potential range of -100 to 1000 mV, equilibrium time of 10 s and scan rate of 30 mV/s. Human serum samples were drawn from a volunteer in our working lab. A written statement informing the consent of the volunteer was received. Clinical studies were performed on the collected human serum and approved by the ethics committee.

3. RESULTS AND DISCUSSION

FESEM was used to characterize and examine the synthesized Pd-doped ZnO NRs on the GCE. As shown in Figure 1, the growth of ZnO as hexagonal nanorods in the direction perpendicular to the GCE surface can be found in samples. After doping with Pd ions, the diameters of the undoped ZnO NRs increased. Reports had been made earlier on how doping influences the ZnO morphology [15]. The diameters of the undoped and Mn-doped ZnO were in the range of 30-60 nm and 70-150 nm, respectively. It is visible that the morphology of the synthesized undoped and Ag-doped ZnO NRs are very high-density rod-shaped structures.

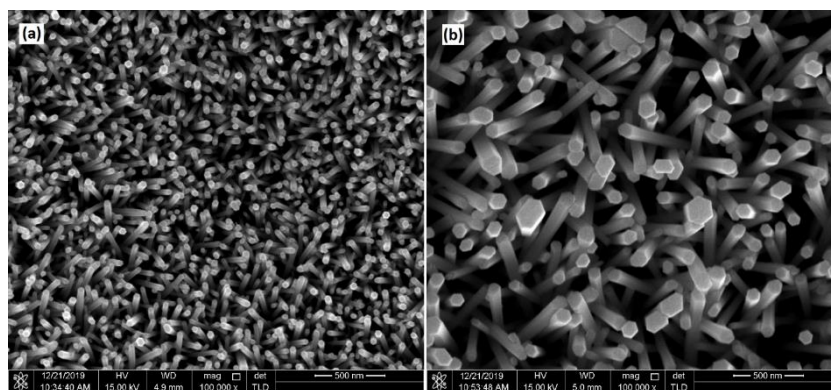


Figure 1. FESEM images of (a) undoped and (b) Pd-doped Zinc oxidenanorodsgrown on GCE using the chemical bath deposition method at 95 °C growth temperaturefor 3 hours.

Thus, the synthesis of dense homogenous ZnO structures with a high aspect ratio is effective when done by chemical method, which holds good for electrochemical sensor applications that have high sensitivity and selectivity.

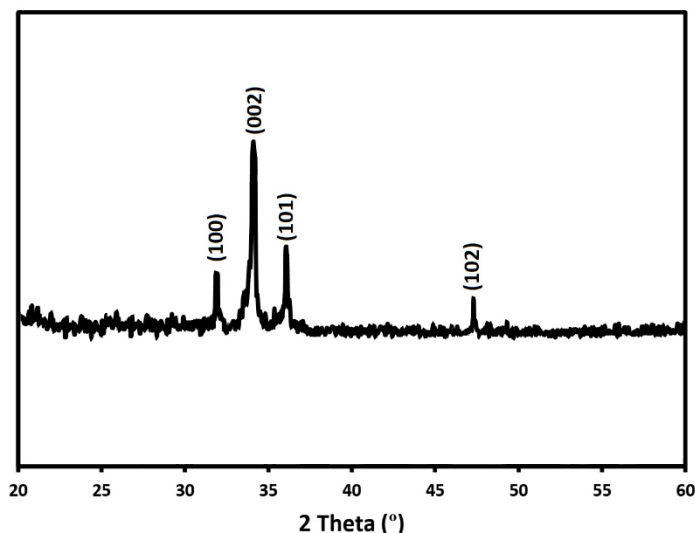


Figure 2. XRD pattern of the Pd-doped ZnO nanorods

The XRD pattern of the Pd-doped ZnO nanorods is shown in figure 2. The pattern shows only peaks that can be matched to hexagonal wurtzite ZnO structure (JCPDS No. 36 - 1451) [16], without secondary peaks from probable elements like Pd oxides.

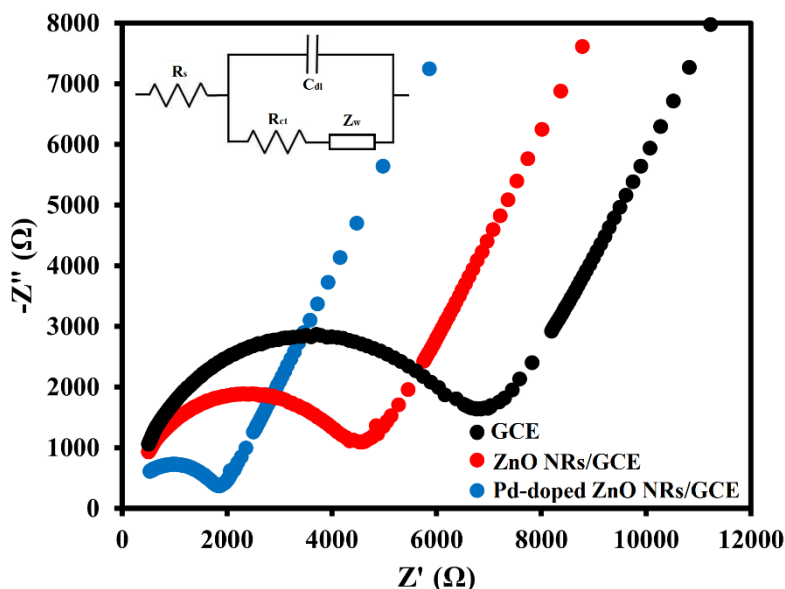


Figure 3. Nyquist plots of bare GCE, ZnO NRs/GCE, and Pd-doped ZnO NRs/GCE electrodes in a combination of 0.5 M H₂SO₄ and 0.1 M KOH solutions under 0.5 V. The inset shows Randles equivalent circuit model.

Figure 3 indicates the impedance spectra of various electrodes fabricated. EIS measurements were done in a combination of 0.5 M sulfuric acid and 0.1 M potassium hydroxide solution to monitor the electrochemical behavior of the electrodes. The impedance results were received by the employed Randles equivalent circuit as shown in Figure 3 inset [17]. The bare GCE electrode displays the semicircle with the largest radius with the 7850 Ω charge transfer resistance (R_{ct}). But the radius decreases with an increase in growth of nanorods on the GCE, along with the decline in R_{ct}, the value

is showing an enhanced rate of electron transfer [18]. To select the electrode with the highest efficiency, the grown zinc oxide nanorods on GCE were modified by dipping them in Pd. As shown in figure 3, the Pd-doped ZnONanorods/GCE electrode displayed an enhanced rate of electron transfer. The best values of R_{ct} , 1950Ω were obtained for zinc oxide nanorods after dipping. Therefore, the Pd-doped ZnO NRs/GCE electrode was chosen to perform additional electrochemical characterization and to be used to detect glucose.

EIS is widely used to get data on the surface characteristics of electrodes [19]. Besides, the rate of electron transfer between the electrolyte and the electrode surface can be seen using EIS [20]. Figure 4 shows the Nyquist plots of Pd-doped zinc oxide nanorods/GCE in 0.1 M potassium hydroxide solution to detect various concentrations of glucose. It can be seen that the increase in glucose concentration reduces the radius of the semicircles. This is because of the glucose and the sensing membranes interacting with each other [21]. Adding glucose causes important changes in the impedance at low frequencies.

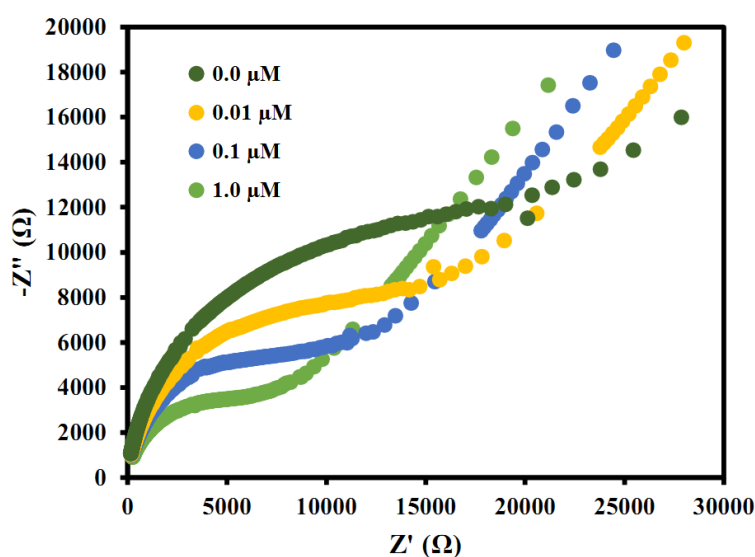


Figure 4. Nyquist plots of Pd-doped ZnO NRs/GCE electrode in 0.1 M KOH solutions for varying concentrations of glucose.

Figure 5a shows the impact of the scan rate on the routine of the cyclic voltammetry of the Pd-doped zinc oxide NRs/GCE electrode. The change in scan rate ranging from 10 to 200 mV/s, causing an increase in the currents of both the oxidation and the reduction peaks. The relation between the scan rate and the peak current is expressed as $i_p = 2.69 \times 10^5 n^{3/2} D^{1/2} v^{1/2} A c$ [22], in which the number of exchanged electrons is represented by n , the diffusion coefficient of reactant is represented by D , the scan rate is represented by v , the effective area of the electrode, and the reactant concentration are represented respectively by A and c . Seemingly, the increase in scan rate rises the peak current and is found to be proportionate to the square root of the scan rate (figure 5b). This shows that the Pd-doped zinc oxide NRs/GCE electrode had undergone a diffusion-controlled electrochemical process. So, the diffusion

process significantly controlled the electrochemical reaction and a huge part of the reaction time was occupied by the diffusion of the analyte.

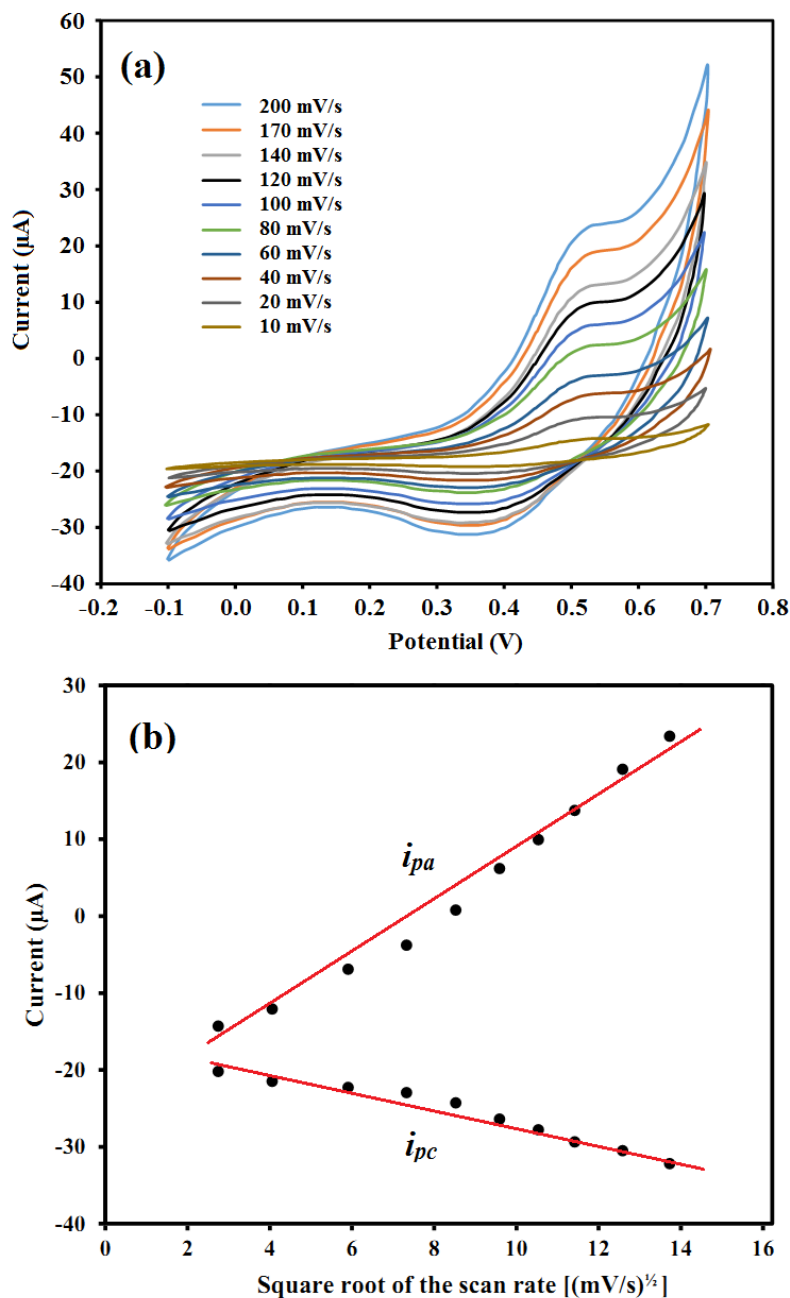


Figure 5. (a) CVs of the Pd-doped ZnO NRs/GCE glucose sensor at scan rates of 10-200 mV/s(b) The plots of the peak currents of the anode and cathode versus the square root of the scan rate.

Even though doping the zinc oxide NRs with Pd had flattened the surface a little along with the reduction of hydrophilic nature in zinc oxide NRs and reducing the area of contact of the solid-liquid interface, it incredibly enhanced the capability of the Pd-doped zinc oxide NRs to transfer electrons. Hence, the sensor fabricated using these NRs are anticipated to have increased performance.

Differential pulse voltammetry (DPV) experiments were done for different concentrations of glucose. Figure 6 illustrates the typical DPV response upon successive add-ons of glucose at Pd-doped ZnO NRs/GCE. It can be seen that the Pd-doped ZnO NRs/GCE reaches a steady-state current, indicating the designed sensor has a quick response to glucose [23]. There exists a linear relation between the current response and the varying concentrations of glucose ranging from 1-800 μM . The linear regression equation can be expressed as: $I (\mu\text{A}) = 0.6453C (\mu\text{M}) + 3.78562$ ($R^2 = 0.9856$). The limit of detection was found to be $0.3\mu\text{M}$. As shown in table 1, the relative study designated that the projected sensor could be practical to detect the glucose content with high sensitivity.

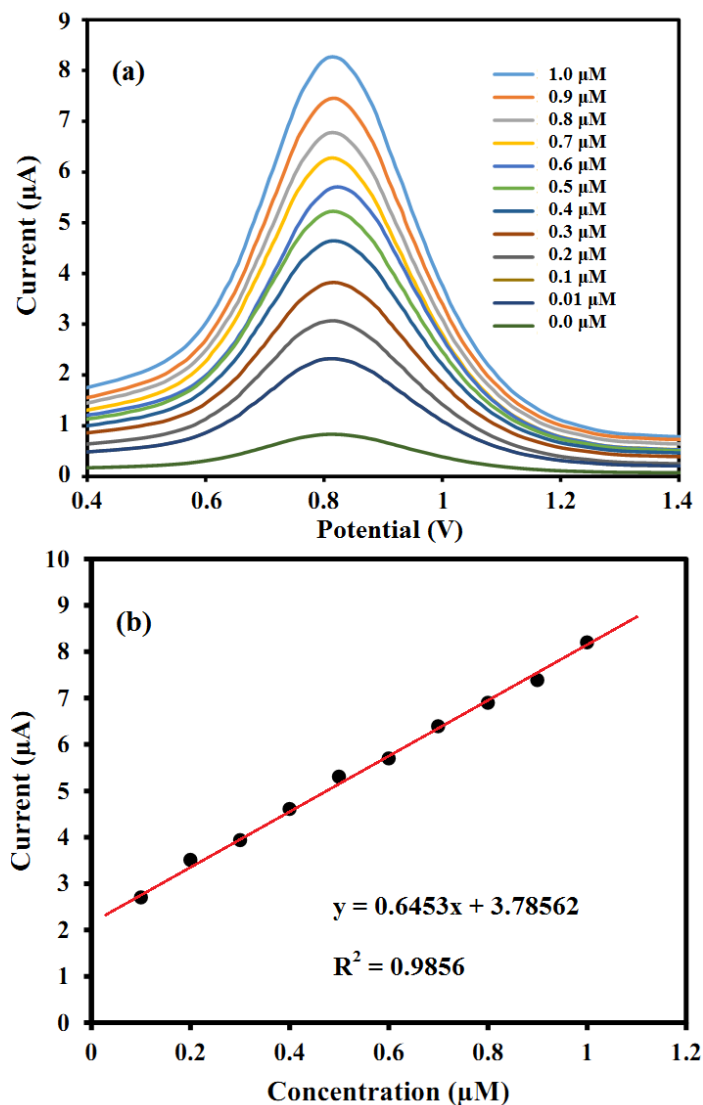


Figure 6. (a) DPVs of Pd-doped ZnO NRs /GCE electrode (b) Calibration plot of the linear variation of DPV peak current in varying concentration of glucose at 0.1 M phosphate buffer solution and 30 mV s^{-1} scan rate.

Table 1. Comparison of Pd-doped ZnO NRs/GCE performance with other electrochemical glucose sensors.

Technique	Electrodes	Sensitivity ($\mu\text{A}/\mu\text{Mcm}^2$)	detection limit (μM)	Ref.
Chronoamperometric	MAF-4-Co ^{II} /GCE	30.95	0.6	[24]
Chronoamperograms	FCA/GOx/PAD	0.9474	50	[25]
Amperometry	Lamellar ridge–Au	0.029	0.87	[26]
Chronoamperograms	CoPc/G/IL/SPCE	9.76	0.67	[27]
Amperometry	polynorepinephrine /glucose oxidase/Au NPs	59170	1.76	[28]
CV	DLEG-CuNCs	4532	0.25	[29]
DPV	Pd-doped ZnO NRs/GCE	0.64	0.3	This work

The applicability of the Pd-doped ZnO NRs/GCE electrode for the determination of glucose in the human blood serum was examined. DPVs were employed to perform the tests. Human blood serum was diluted with Phosphate buffer solution to measure. Concentrations were estimated by using a calibration plot by the standard addition method [30]. Every appropriate measurement was done thrice without pretreatment employing the standard addition method. The results are displayed in Table 2. Recovery studies were also done using the blood serum, and recoveries were ranging between 99.61% and 102.75% for glucose. The results show that the Pd-doped ZnO NRs/GCE electrode can be favorably employed to determine glucose in blood serum samples under the optimized conditions using the standard addition method.

Table 2. Determination of glucose in human blood serum with Pd-doped ZnO NRs/GCE

Sample	Added concentration (μMl^{-1})	Found concentration (μMl^{-1})	Recovery (%)	RSD (%)
1	70	70.23	100.53	2.23
2	80	79.24	99.61	2.39
3	90	91.76	102.42	1.67
4	100	101.52	102.75	1.62

4. CONCLUSIONS

A novel Pd-doped ZnO NRs material was synthesized on GCE and used to prepare a selective and sensitive electrochemical glucose sensor. The structural properties of Pd-doped ZnO NRs were characterized by SEM and XRD. The Pd-doped ZnO NRs/GCE possessed excellent electrochemical features in glucose detection, due to the Pd-doped ZnO NRs had improved the surface area. The developed sensor was considered to be highly selective and sensitive to glucose with a detection limit of 0.3 μM and a sensitivity of 0.64 $\mu\text{A}/\mu\text{Mcm}^2$. Furthermore, this electrochemical sensor indicated a good reliability, reproducibility and stability measurements in human blood samples.

ACKNOWLEDGEMENT

This work was sponsored in part by Guided Innovation Fund of Northeast Petroleum University (2019QNQ-09).

References

1. L. Jin, Z. Meng, Y. Zhang, S. Cai, Z. Zhang, C. Li, L. Shang and Y. Shen, *ACS applied materials & interfaces*, 9 (2017) 10027.
2. N.X. Viet, M. Chikae, Y. Ukita and Y. Takamura, *International Journal of Electrochemical Science*, 13 (2018) 8633.
3. L. Xie, A.M. Asiri and X. Sun, *Sensors and Actuators B: Chemical*, 244 (2017) 11.
4. E.F. Gabriel, P.T. Garcia, T.M. Cardoso, F.M. Lopes, F.T. Martins and W.K. Coltro, *Analyst*, 141 (2016) 4749.
5. H. Yang, C. Gong, L. Miao and F. Xu, *International Journal of Electrochemical Science*, 12 (2017) 4958.
6. J. Peng and J. Weng, *Biosensors and Bioelectronics*, 89 (2017) 652.
7. Y. Sun, Y. Li, N. Wang, Q.Q. Xu, L. Xu and M. Lin, *Electroanalysis*, 30 (2018) 474.
8. X. Fu, Z. Chen, S. Shen, L. Xu and Z. Luo, *International Journal of Electrochemical Science*, 13 (2018) 4817.
9. Y. Dai, A. Molazemhosseini, K. Abbasi and C.C. Liu, *Biosensors*, 8 (2018) 4.
10. F. Husairi, J. Rouhi, K. Eswar, A. Zainurul, M. Rusop and S. Abdullah, *Applied Physics A*, 116 (2014) 2119.
11. J. Rouhi, S. Mahmud, S.D. Hutagalung and S. Kakooei, *Journal of Micro/Nanolithography, MEMS, and MOEMS*, 10 (2011) 043002.
12. Y. Yang, Y. Wang, X. Bao and H. Li, *Journal of Electroanalytical Chemistry*, 775 (2016) 163.
13. F. Husairi, J. Rouhi, K. Eswar, C.R. Ooi, M. Rusop and S. Abdullah, *Sensors and Actuators A: Physical*, 236 (2015) 11.
14. A. Mahmoud, M. Echabaane, K. Omri, L. El Mir and R.B. Chaabane, *Journal of Alloys and Compounds*, 786 (2019) 960.
15. M. Samadi, M. Zirak, A. Naseri, E. Khorashadizade and A.Z. Moshfegh, *Thin Solid Films*, 605 (2016) 2.
16. R. Dalvand, S. Mahmud and J. Rouhi, *Materials Letters*, 160 (2015) 444.
17. S.S. Ghoreishizadeh, X. Zhang, S. Sharma and P. Georgiou, *IEEE sensors letters*, 2 (2017) 1.
18. J. Rouhi, S. Kakooei, M.C. Ismail, R. Karimzadeh and M.R. Mahmood, *International Journal of Electrochemical Science*, 12 (2017) 9933.
19. M. Xu, X. Luo and J.J. Davis, *Biosensors and Bioelectronics*, 39 (2013) 21.
20. Q. Wang, H. Dong and H. Yu, *Journal of Power Sources*, 271 (2014) 278.
21. P. Theurey and J. Rieusset, *Trends in Endocrinology & Metabolism*, 28 (2017) 32.
22. Y. Shi, L. Wen, F. Li and H.-M. Cheng, *Journal of Power Sources*, 196 (2011) 8610.
23. R. Li, X. Liu, H. Wang, Y. Wu, K. Chan and Z. Lu, *Electrochimica Acta*, 299 (2019) 470.
24. N.S. Lopa, M.M. Rahman, F. Ahmed, T. Ryu, J. Lei, I. Choi, D.H. Kim, Y.H. Lee and W. Kim, *Journal of Electroanalytical Chemistry*, 840 (2019) 263.
25. W. Li, D. Qian, Q. Wang, Y. Li, N. Bao, H. Gu and C. Yu, *Sensors and Actuators B: Chemical*, 231 (2016) 230.
26. X. Guo, H. Deng, H. Zhou, T. Fan and Z. Gao, *Sensors and Actuators B: Chemical*, 206 (2015) 721.
27. S. Chaiyo, E. Mehmeti, W. Siangproh, T.L. Hoang, H.P. Nguyen, O. Chailapakul and K. Kalcher, *Biosensors and Bioelectronics*, 102 (2018) 113.

28. Y. Liu, X. Nan, W. Shi, X. Liu, Z. He, Y. Sun and D. Ge, *RSC Advances*, 9 (2019) 16439.
29. F. Tehrani and B. Bavarian, *Scientific reports*, 6 (2016) 1.
30. M.A. Papi, M.F. Bergamini and L.H. Marcolino-Junior, *Journal of Electroanalytical Chemistry*, 835 (2019) 248.

© 2020 The Authors. Published by ESG (www.electrochemsci.org). This article is an open access article distributed under the terms and conditions of the Creative Commons Attribution license (<http://creativecommons.org/licenses/by/4.0/>).